

The Clathrin Adaptor AP-1A Mediates Basolateral Polarity

Diego Gravotta,^{1,*} Jose Maria Carvajal-Gonzalez,^{1,5} Rafael Mattera,^{4,5} Sylvie Deborde,¹ Jason R. Banfelder,² Juan S. Bonifacino,⁴ and Enrique Rodriguez-Boulan^{1,3,*}

¹Margaret Dyson Vision Research Institute, Department of Ophthalmology

²Department of Physiology and Biophysics

³Department of Cell and Developmental Biology

Weill Cornell Medical College, New York, NY 10065, USA

⁴Cell Biology and Metabolism Program, Eunice Kennedy Shriver National Institute of Child Health and Human Development, National Institutes of Health, Bethesda, MD 20892, USA

⁵These authors contributed equally to this work

*Correspondence: dig2003@med.cornell.edu (D.G.), boulan@med.cornell.edu (E.R.-B.)

DOI 10.1016/j.devcel.2012.02.004

SUMMARY

Clathrin and the epithelial-specific clathrin adaptor AP-1B mediate basolateral trafficking in epithelia. However, several epithelia lack AP-1B, and mice knocked out for AP-1B are viable, suggesting the existence of additional mechanisms that control basolateral polarity. Here, we demonstrate a distinct role of the ubiquitous clathrin adaptor AP-1A in basolateral protein sorting. Knockdown of AP-1A causes missorting of basolateral proteins in MDCK cells, but only after knockdown of AP-1B, suggesting that AP-1B can compensate for lack of AP-1A. AP-1A localizes predominantly to the TGN, and its knockdown promotes spillover of basolateral proteins into common recycling endosomes, the site of function of AP-1B, suggesting complementary roles of both adaptors in basolateral sorting. Yeast two-hybrid assays detect interactions between the basolateral signal of transferrin receptor and the medium subunits of both AP-1A and AP-1B. The basolateral sorting function of AP-1A reported here establishes AP-1 as a major regulator of epithelial polarity.

INTRODUCTION

Epithelial cells perform key vectorial functions in secretion and absorption that depend on the accurate localization of transporters, channels, and receptors to apical and basolateral domains (Philp et al., 2011). Sorting of plasma membrane proteins occurs in both biosynthetic and recycling routes through recognition of apical and basolateral sorting signals by machinery in the *trans*-Golgi network (TGN) and common recycling endosomes (CREs) (Bryant and Mostov, 2008; Mellman and Nelson, 2008; Rodriguez-Boulan et al., 2005). Whereas apical sorting signals and mechanisms are complex, basolateral sorting requires simple sorting signals, in some cases similar to those used by clathrin-mediated endocytosis (Gonzalez and Rodriguez-Boulan, 2009; Traub, 2009; Weisz and Rodriguez-Boulan,

2009). Like clathrin-mediated endocytosis, basolateral trafficking requires clathrin (Deborde et al., 2008) and clathrin-associated sorting proteins, such as the heterotetrameric adaptor AP-1B (Fölsch et al., 1999; Ohno et al., 1999) to coordinate the recruitment of cargo proteins via their sorting signals with the formation of clathrin-coated vesicles. However, many aspects of clathrin-mediated basolateral sorting remain unclear (Mostov et al., 1999), particularly the interactions of basolateral sorting signals with AP-1B, which contrasts with the detailed knowledge available on the interactions of the plasma membrane adaptor AP-2 with endocytic sorting signals (Janvier et al., 2003; Kelly et al., 2008; Owen and Evans, 1998; Traub, 2009).

Independent lines of evidence suggest that clathrin-mediated basolateral sorting requires additional adaptors besides the epithelial-specific AP-1B. Recent work has confirmed that several native epithelia constitutively lack AP-1B, e.g., liver (Ohno et al., 1999), retinal pigment epithelium (Diaz et al., 2009), and kidney proximal tubule (Schreiner et al., 2010). Furthermore, mice depleted of AP-1B through knockout (KO) of the medium (μ 1B) subunit are viable, albeit they develop colon inflammation due to apical mislocalization of cytokine receptors (Takahashi et al., 2011). Thus, epithelia, the majority of the ~200 estimated cell types in the human body (Alberts, 2002), must have additional, not yet identified, mechanisms controlling basolateral trafficking that allow survival of the organism in the absence of AP-1B. Given the requirement for clathrin in basolateral trafficking (Deborde et al., 2008), these may likely be found among ~20 clathrin-associated sorting proteins known to coordinate with clathrin various intracellular trafficking processes (Bonifacino and Traub, 2003). Another heterotetrameric adaptor complex, AP-4, has been implicated in basolateral polarity (Simmen et al., 2002), but this adaptor does not interact with clathrin (Bonifacino and Traub, 2003) and its basolateral sorting role has not been confirmed by other studies.

The ubiquitous clathrin-associated heterotetrameric adaptor AP-1A is a strong candidate to play a role in epithelial polarity. AP-1A shares three subunits with AP-1B (γ , β 1, σ 1), differing only in the possession of a different medium subunit, μ 1A instead of μ 1B (Ohno et al., 1999). AP-1 KO is embryonic lethal in multicellular organisms, e.g., *Caenorhabditis elegans* (Lee et al., 1994) and mouse (Zizioli et al., 1999). Whereas γ -adaptin KO blocks mouse development at the morula stage (day 2–3 postcoitus [pc]) (Zizioli et al., 1999), μ 1A KO stops development at the start

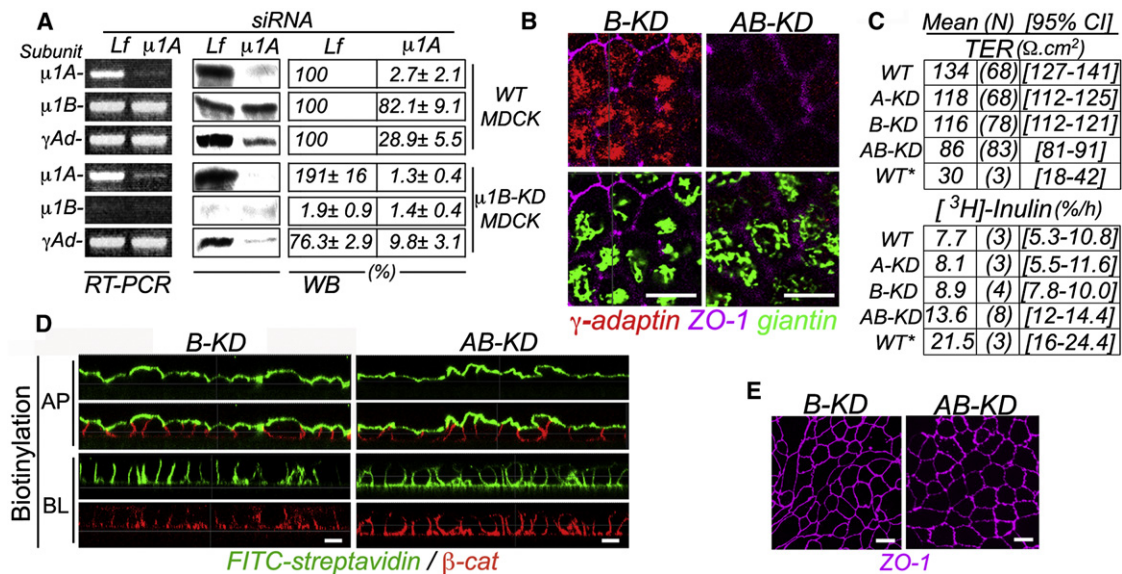


Figure 1. Single and Double Knockdown of AP-1A and AP-1B in MDCK Cells

MDCK cells, wild-type (WT) or permanently depleted of μ 1B with shRNA (μ 1B-KD) (Gravotta et al., 2007), were transfected by electroporation with control siRNA targeting luciferase (Lf) or μ 1A siRNA for three consecutive times (at 3 day intervals each; see Experimental Procedures) and studied 84 hr after the third transfection.

(A) RT-PCR (200 ng RNA input) and western blot (WB, 125 μ g protein/lane); values expressed as percentage of WT MDCK represent average \pm SEM of three independent experiments. Expression in μ 1A siRNA-transfected, relative to Lf siRNA-transfected MDCK cells consistently demonstrated >90% reduction of μ 1A in both WT and B-KD MDCK cells ($p < 1.4 \times 10^{-6}$ and 1.0×10^{-9}). A-KD cells had no compensatory increase of μ 1B (Figure 1A; $p < 0.12$), unlike B-KD cells which exhibited increased μ 1A levels (Figure 1A; $p < 0.004$), as previously shown (Gravotta et al., 2007). RT-PCR analysis did not detect any decrease in γ -adaptin mRNA levels in A-KD, B-KD, or AB-KD cells, whereas western blotting detected decreases in protein levels of \sim 71% ($p < 2.0 \times 10^{-4}$), 25% ($p < 0.0012$), or 92% ($p < 8.3 \times 10^{-6}$), respectively, relative to WT MDCK cells.

(B) Immunofluorescence microscopy in permeabilized AB-KD MDCK cells confirmed the strong reduction of γ -adaptin in the perinuclear region, highlighted by staining of the Golgi-resident protein giantin. Bar, 12 μ m.

(C) The *trans*-epithelial electrical resistance (TER) was slightly decreased, in A-KD (12%, $p < 1 \times 10^{-3}$), and B-KD (14%, $p < 6 \times 10^{-5}$) MDCK cells, and moderately decreased in AB-KD (30%, $p < 2 \times 10^{-16}$) MDCK cells compared to WT MDCK cells, although considerably less than in WT MDCK cells treated with Ca, Mg-free HBSS for 1.5 hr (WT*) (78%, $p = 2 \times 10^{-8}$). Inulin permeability was not significantly reduced, relative to WT MDCK cells (7.7% leaked to the opposite chamber) in A-KD (8%, $p < 1$) or B-KD (8.9%, $p < 0.79$) but was significantly reduced in AB-KD (13.6%, $p < 2 \times 10^{-6}$) MDCK cells. Values shown represent the means of the indicated number of independent measurements (N) and 95% confidence interval (CI). For statistical analysis, see Table S1.

(D) Domain selective biotinylation of MDCK monolayers grown on polycarbonate filters demonstrate preservation of TJ, as assessed by staining with FITC-streptavidin from the apical or basolateral side (see Experimental Procedures for details). Bar, 12 μ m.

(E) The morphology of tight junctions was normal in B-KD and AB-KD MDCK cells as revealed by immunostaining of ZO-1. Bar, 12 μ m.

of epithelial organogenesis (day 13.5 pc), indicating that AP-1B can compensate partially for the absence of AP-1A (Meyer et al., 2000). Conversely, the viability of AP-1B KO mice (Takahashi et al., 2011) suggests that AP-1A can compensate for AP-1B function. That AP-1A and AP-1B can compensate for each other asymmetrically during mouse development suggests a role for AP-1A in epithelial polarity, complementary to that of AP-1B.

Here we report a role of AP-1A in basolateral protein sorting at the TGN, complementary to the established basolateral sorting role of AP-1B at recycling endosomes. Together with the reported requirement of AP-1 for dendritic polarization in neurons (Dwyer et al., 2001), these results establish AP-1 as a key regulator of polarized trafficking.

RESULTS

Single and Double Knockdown of AP-1A and AP-1B in MDCK Cells

We identified a potent and specific silencing sequence for canine μ 1A (μ 1A-siRNA) and used it to generate four populations of

MDCK cells by Amaxa electroporation (see Experimental Procedures); WT or control (wild-type MDCK cells transfected with Luciferase-siRNA), A-KD (WT MDCK cells transfected with μ 1A-siRNA), B-KD (μ 1B-KD MDCK cells transfected with Lf-siRNA), and AB-KD (μ 1B-KD MDCK cells transfected with μ 1A-siRNA). RT-PCR and western blot (WB) analysis revealed efficient silencing (>90%) of μ 1A mRNA and protein in A-KD and AB-KD cells. Whereas B-KD cells exhibited significantly increased μ 1A, as previously shown (Gravotta et al., 2007), A-KD cells did not show compensatory increase or decrease of μ 1B (Figure 1A). γ -adaptin mRNA levels did not change in A-KD, B-KD, or AB-KD cells (Figure 1A, RT-PCR); in contrast, γ -adaptin protein levels were significantly decreased in B-KD (24%), A-KD (71%), and AB-KD (92%) MDCK cells (Figure 1A, WB; Figure 1B, immunofluorescence). AB-KD MDCK cells also exhibited a drastic decrease in the level of β -adaptin subunit (see Figure S1 available online), consistent with previous reports indicating that adaptor protein subunits not incorporated into fully assembled adaptors are targeted for degradation (Meyer et al., 2000; Zizioli et al., 1999).

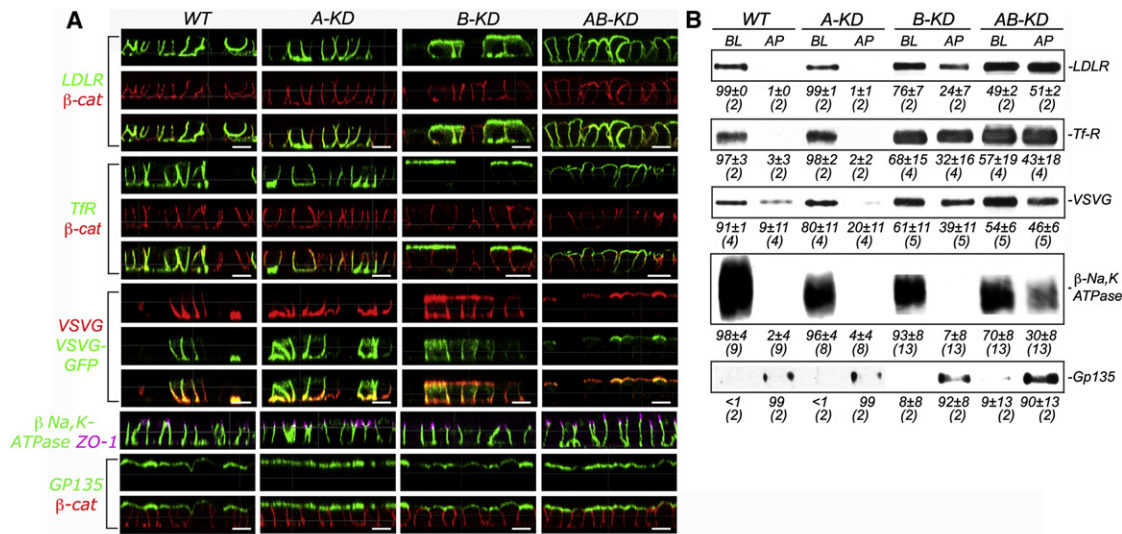


Figure 2. Steady-State Distribution of Polarity Markers in A-KD, B-KD, and AB-KD MDCK Cells

A-KD, B-KD, and AB-KD MDCK cells, generated as described in the legend to Figure 1 and plated on polycarbonate filters, were analyzed for the polarized distribution of several endogenous and exogenous PM markers by (A) immunofluorescence or (B) domain-selective biotinylation, streptavidin-agarose retrieval and western blotting. The distributions of LDL receptor (LDLR), transferrin receptor (TfR) and GFP-tagged vesicular stomatitis virus G protein (VSVG-GFP) were monitored in cell monolayers transduced with the respective adenoviruses 50–54 hr after plating and processed for immunofluorescence 26–30 hr later (for details, see *Experimental Procedures*). The remaining markers (NaK-ATPase, β -catenin, and gp135) were all endogenous to MDCK cells.

(A) Immunofluorescence and confocal microscopy. Cell surface immunolabeling was performed on paraformaldehyde-fixed monolayers grown on Transwell chambers, incubated with the respective antibodies to the PM proteins added to both apical and basolateral domains followed by a secondary antibody (shown in green for all proteins except for VSVG-GFP displayed in red). In a second step, cells were permeabilized with saponin to decorate β -catenin or ZO-1 with specific antibodies (shown in red and purple, respectively). Samples were analyzed using a Leica SP2 scanning confocal microscope and images are displayed as x-z sections. Bar, 12 μ m.

(B) Domain-selective biotinylation. Cell surface proteins, subjected to domain-selective biotinylation from the apical (AP) or basolateral (BL) domains and recovered by streptavidin-agarose from cell lysates were analyzed by SDS-PAGE followed by western blotting. Proteins identified with their respective antibodies, were visualized by chemiluminescence and quantified by NIH-imaging software. Values represent the means \pm SD of the number of independent experiments shown between parentheses. Note that B-KD and AB-KD (but not A-KD) MDCK cells display loss of polarity of LDLR, TfR and VSVG protein. In contrast, NaK-ATPase polarity is only moderately reduced in AB-KD MDCK cells, whereas the apical PM protein gp135 remains apically polarized under all experimental conditions.

Other experiments showed that tight junction (TJ) structure and function were preserved in A-KD, B-KD, and AB-KD MDCK cells (Figures 1C and 1E; see *Table S1* for statistical analysis). Fluorescein isothiocyanate (FITC)-streptavidin decoration of biotinylated monolayers showed selective labeling only of the biotin-exposed domain (Figure 1D), consistent with the reported impermeability of TJ to negatively charged molecules (Moreno and Diamond, 1974). These experiments validate the various biotin-based polarity assays used in this article to study the roles of AP-1A and AP-1B in the sorting of basolateral membrane proteins.

Double Knockdown of AP-1A and AP-1B Causes a Drastic Loss of Basolateral Plasma Membrane Protein Polarity

We studied the effect of A-KD, B-KD, and AB-KD on the steady-state localization of basolateral and apical markers in polarized MDCK cells using confocal microscopy (Figure 2A) and quantitative domain-selective biotinylation (Figure 2B). In agreement with previous studies (Gravotta et al., 2007), we found that B-KD decreased significantly the steady-state basolateral polarity of transferrin receptor (TfR) (68% versus WT 97%), LDL receptor (LDLR) (76% versus WT 99%), and vesic-

ular stomatitis virus G protein (VSVG) (61% versus WT 91%), all expressed via adenoviruses. In contrast, A-KD did not affect or affected only slightly the basolateral polarity of these markers (98%, 99%, and 80%, respectively). Strikingly, AB-KD disrupted the steady-state basolateral polarity of these markers to a larger extent than B-KD alone (57%, 49%, 54%, respectively) (Figures 2A and 2B).

The polarity of two endogenous plasma membrane (PM) proteins, E-cadherin and β 1-integrin, was drastically disrupted by AB-KD but not by A-KD or B-KD (data not shown). Na,K-ATPase, 98% basolateral in WT cells, was not affected by A-KD or B-KD (96% and 93% basolateral, respectively) and was slightly depolarized by AB-KD (70% basolateral). The polarity of the apical PM protein GP135 was not impacted by KD of either one or both adaptors (99% apical in WT and A-KD, 92% apical in B-KD, and 90% apical in AB-KD MDCK cells).

The drastic loss of polarity of several basolateral PM proteins in AB-KD cells contrasted with the mild loss of polarity in B-KD cells and the silent phenotype of A-KD cells, suggesting that AP-1A has a role in basolateral polarity distinct from that of AP-1B. These results further suggest that AP1A and AP1B sorting roles are asymmetric, with AP-1B capable of compensating for the absence of AP-1A, but not vice versa.

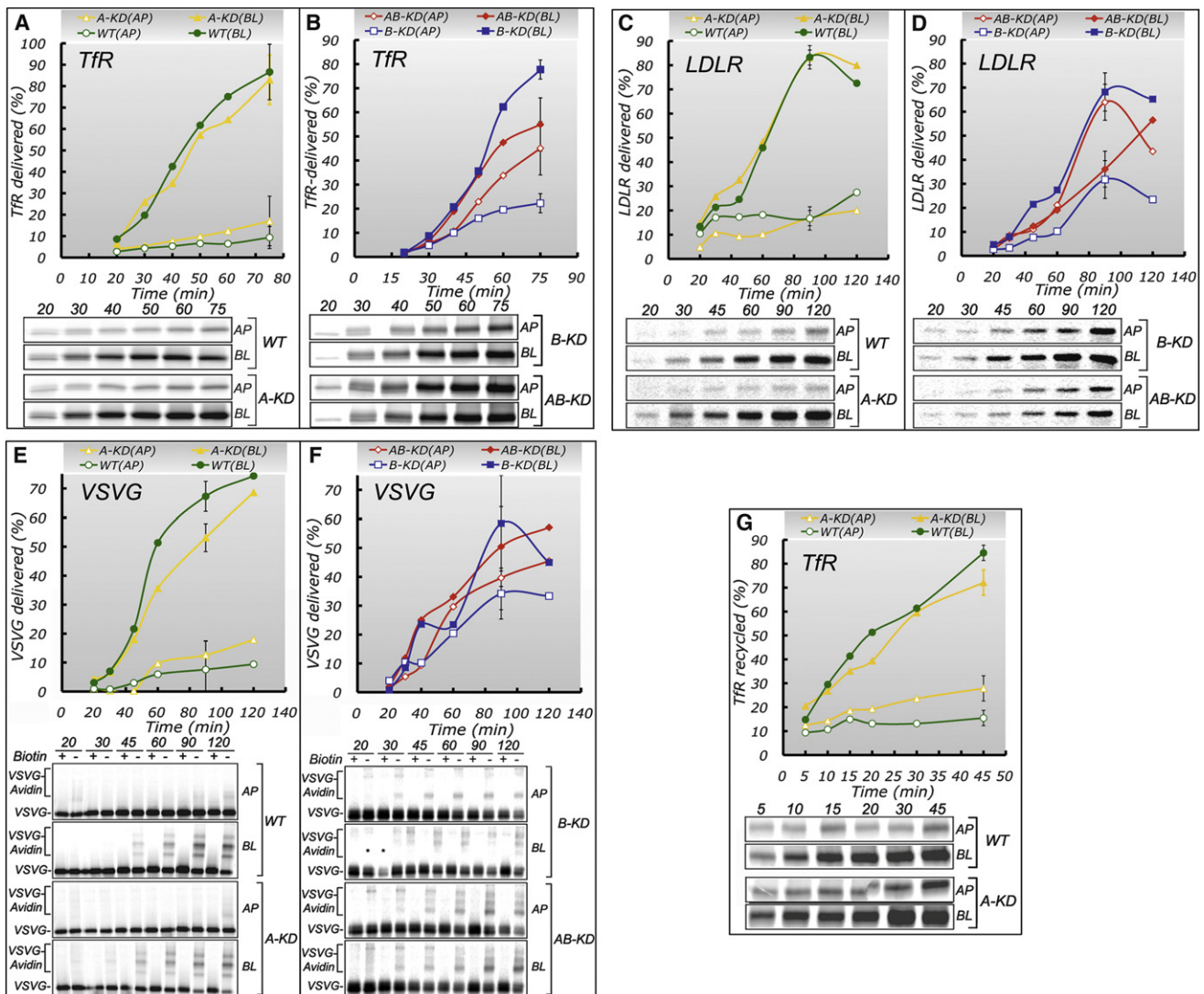


Figure 3. Effect of AP-1A and AP-1B Knockdown on the Biosynthetic Delivery and Recycling of Basolateral PM Proteins

(A-F) Biosynthetic sorting of several basolateral PM proteins was studied in A-KD, B-KD, and AB-KD MDCK cells confluent on polycarbonate filters for 84 hr, as detailed in [Experimental Procedures](#). The surface arrival of indicated [³⁵S]-labeled newly synthesized proteins was measured in cells transfected with adenoviruses encoding hTfr, hLDLR, or VSVG-GFP, using, ligand capture (Tfr) (A and B), surface immunoprecipitation (LDLR) (C and D) or surface biotinylation-avidin shift assay (VSVG) (E and F) (see [Experimental Procedures](#) for details). Time points showing standard deviation bars represent the average of four to six independent experiments; these data and their statistical analysis by ANOVA along with the Bonferroni and Holm corrections for multiple comparisons are shown in [Table S2](#).

(G) The recycling of Tfr was studied using a modification of the ligand-capture assay used to measure biosynthetic delivery (see [Experimental Procedures](#)) in WT and A-KD MDCK cells. Each time point represents the average of at least two independent experiments. The 45 min time point, showing standard deviation bars, represents the average of four to six independent experiments. These data and their statistical analysis by ANOVA along with the Bonferroni and Holm corrections for multiple comparisons are shown in [Table S2](#).

Double Knockdown of μ 1A and μ 1B Causes Missorting of Newly Synthesized Tfr and LDR

The polarized steady-state distribution of PM proteins reflects the amounts delivered by their biosynthetic and recycling pathways to each PM domain. Previous work has shown that Tfr and LDLR move along biosynthetic pathways from TGN to the basolateral PM ([Cancino et al., 2007; Gan et al., 2002; Gravotta et al., 2007](#)), whereas VSVG protein utilizes a specialized biosynthetic route through CREs, the site of function of AP-1B ([Ang](#)

[et al., 2004; Cancino et al., 2007; Gravotta et al., 2007](#)). To dissect a possible role of AP-1A in basolateral trafficking, we studied the effect of A-KD, B-KD, and AB-KD on the biosynthetic delivery of Tfr, LDLR, and VSVG protein ([Figure 3; see Table S2](#) for values and statistical analysis). We found that AB-KD MDCK cells dramatically disrupted the polarized biosynthetic delivery of LDLR (WT 79%; AB-KD 36% basolateral) and Tfr (WT 91%; AB-KD 52% basolateral), whereas A-KD and B-KD caused a more moderate disruption (LDLR A-KD 79%; B-KD 71%

basolateral) (TfR A-KD 79%; B-KD 74%) (Figures 3A–3D). In contrast with these results, B-KD, but not A-KD, drastically disrupted the biosynthetic route of VSVG protein and AB-KD did not cause additional missorting beyond that caused by B-KD (Figures 3E and 3F; see Table S2 for statistical analysis). Taken together, these experiments indicate that both AP-1A and AP-1B are required for accurate biosynthetic sorting of LDLR and TfR, whereas AP-1B, but not AP-1A, is required for biosynthetic sorting of VSVG protein.

AP-1A Does Not Mediate Recycling of Endocytosed Transferrin Receptor

We have previously shown that LLC-PK1 cells (which constitutively lack AP-1B) or B-KD MDCK cells missort LDLR or TfR receptor in the recycling route, consistent with the postulated sorting role and localization of AP-1B at CRE (Ang et al., 2004; Cancino et al., 2007; Fölsch et al., 2003; Gan et al., 2002; Gravotta et al., 2007). Here, we studied the effect of A-KD on the recycling of TfR, using an adaptation of the ligand capture assay described in Experimental Procedures. A-KD did not disrupt polarized TfR recycling (Figure 3G; Table S2), in striking contrast with B-KD, which caused a profound disruption of TfR recycling, as previously shown (Gravotta et al., 2007).

These results demonstrate that, unlike AP-1B, AP-1A does not mediate recycling of endocytosed proteins. Together with our previous data, these results suggest that AP-1A and AP-1B mediate basolateral protein sorting at different cellular compartments.

AP-1A and AP-1B Localize Preferentially at TGN and CRE, Respectively

To obtain insight on the site of function of AP-1A, we performed a quantitative analysis of the localization of AP-1A and AP-1B in polarized MDCK cells. Previous data in nonpolarized cells indicate that AP-1A localizes and functions at the level of the TGN (Doray et al., 2002; Puertollano et al., 2001; Waguri et al., 2003), and studies in subconfluent epithelial cells (LLC-PK1 and FRT cells) suggest that AP-1A localizes to TGN and AP-1B to CRE (Cancino et al., 2007; Fölsch et al., 2003; Gan et al., 2002). TGN and CRE have partially overlapping distributions in the perinuclear region, which increases the difficulty of these studies (Cancino et al., 2007; Fölsch et al., 2003; Gan et al., 2002). As antibodies capable of detecting endogenous μ 1A and μ 1B by immunofluorescence in MDCK cells are not available, we transiently transfected hemagglutinin-tagged μ 1A (μ 1A-HA) or μ 1B (μ 1B-HA) into WT MDCK cells (Figure 4). Control experiments indicated that ~50% of exogenous μ 1A-HA and μ 1B-HA colocalized with endogenous γ -adaptin, consistent with their efficient integration into the AP-1 complex (Figures 4A and 4D). Consistently, a large proportion of the endogenous γ -adaptin colocalized with μ 1A-HA or μ 1B-HA (Figures 4A and 4E).

μ 1A-HA colocalized more prominently with TGN38 (M1 0.294 ± 0.025) than μ 1B-HA (M1 0.094 ± 0.010) ($p < 3.5 \times 10^{-10}$) (Figures 4B and 4F). In contrast, μ 1B-HA colocalized more prominently with TfR (M1 0.348 ± 0.016) than μ 1A-HA (M1 0.158 ± 0.015) ($p < 2.8 \times 10^{-13}$) (Figures 4C and 4F).

As a complementary approach, we studied the colocalization of TGN38 with the endogenous γ -adaptin subunit, common to both AP-1A and AP-1B, in B-KD MDCK cells, which express

only AP-1A and in A-KD MDCK cells, which express only AP-1B (Figure 4G). These experiments showed that a substantial and significantly larger proportion of the TGN (labeled with the marker TGN38) colocalized with endogenous γ -adaptin in B-KD than in A-KD MDCK cells ($33.7 \pm 1.2\%$ versus $20.8 \pm 3.4\%$, respectively; $p < 0.0073$).

In summary, quantitative colocalization experiments in polarized MDCK cells indicate that AP-1A localizes predominantly to the TGN and AP-1B to CRE.

AP-1A Supports Exit of LDLR-GFP from the TGN

We recently used a live-imaging approach to show that chronic knockdown of clathrin heavy chain by siRNA or functional knockdown by acute crosslinking of clathrin light chain, delays selectively the exit of several basolateral cargo proteins from the TGN (Deborde et al., 2008). Here, we used a similar approach to study the role of AP-1A or AP-1B in the exit of LDLR-GFP from the TGN, defined by the TGN marker sialyltransferase-red fluorescent protein (ST-RFP). The experiments demonstrate that the exit of LDLR-GFP from the TGN is drastically disrupted in AB-KD cells but proceeds at control rates in both A-KD or B-KD cells (Figure 5; see also Movie S1).

These experiments show that the expression of just AP-1A in MDCK cells is sufficient and necessary for efficient exit of LDLR-GFP from the TGN. This is consistent with previous literature showing that AP-1A facilitates exit from the TGN of a variety of membrane proteins, such as mannose-6-phosphate receptor (Doray et al., 2002; Puertollano et al., 2001; Waguri et al., 2003), VSVG (Chi et al., 2008), and the K-channel Kir 2.1 (Ma et al., 2011). However, our data indicate that AP-1B is also apparently sufficient and necessary for efficient exit of LDLR-GFP from the TGN. This is surprising, as previous evidence indicates that AP-1B mediates basolateral sorting of recycling and newly synthesized proteins at CRE (Ang et al., 2004; Cancino et al., 2007; Fölsch et al., 2003; Gan et al., 2002; Gravotta et al., 2007). Our results suggest that AP-1B exhibits a dynamic behavior that allows, in the absence of AP-1A, relocation to the TGN to participate in cargo exit (see Discussion).

A-KD Increases Trafficking of Basolateral Proteins from TGN into CRE

Taken together, the observations reported so far suggest the hypothesis that the silent steady-state phenotype of A-KD MDCK cells results from compensatory diversion of basolateral proteins into CRE and basolateral sorting by AP-1B. To test this hypothesis, we carried out pulse-chase experiments of TfR, LDLR, and VSVG in WT, A-KD and B-KD MDCK cells and measured the fraction of radioactively labeled protein transported into CRE using a postchase “trapping assay” with recycled HRP-Tf (Figure 6; see Experimental Procedures for detailed protocol). This assay differs from endosomal ablation protocols used by other groups (Ang et al., 2004; Cresawn et al., 2007) in that the crosslinking elicited by HRP/diaminobenzidine (DAB) occurs at the end of, not before, cargo chase into recycling endosomes; this approach may avoid artificial disruption of membrane trafficking dynamics (for discussion, see Henry and Sheff, 2008).

After a 15 min pulse and 2 hr incubation at 20°C (to promote accumulation of cargo proteins in the TGN), transfer to 37°C

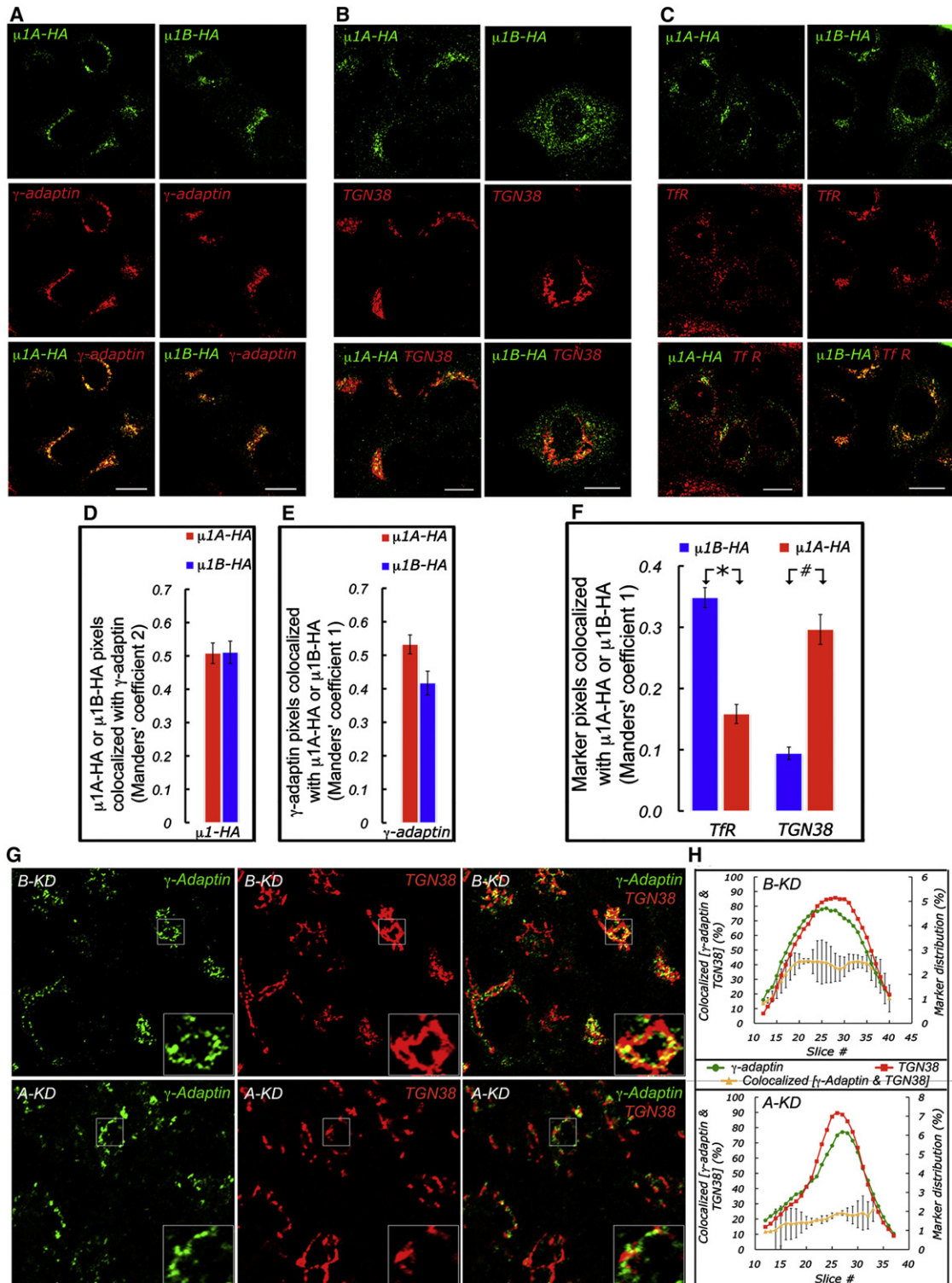


Figure 4. Colocalization of AP-1A and AP-1B with TGN and Recycling Endosome Markers

MDCK cells were transfected with cDNAs encoding μ 1A-HA or μ 1B-HA, cultured as subconfluent monolayers for 72 hr, fixed with paraformaldehyde and permeabilized with saponin and processed for double immunofluorescence and scanning confocal microscopy, as described in *Experimental Procedures*.

(A) Monolayers decorated with antibodies to HA and γ -adaptin demonstrated colocalization of μ 1A and μ 1B with γ -adaptin. Bar, 15 μ m.

(B and C) Cells were immunolabeled with antibodies to influenza HA-tag, TGN38, or transferrin receptor (Tfr). Cells expressing moderate amounts of μ 1A-HA or μ 1B-HA displayed a perinuclear distribution similar to that observed for TGN38 and γ -adaptin. Tfr distributed in both perinuclear and peripheral endosomes. Scale bar = 20 μ m.

for 20 min resulted in progressive accumulation in CRE of up to ~30% of TfR and LDLR in WT MDCK (Figure 6). Strikingly, in A-KD MDCK, the proportion of LDLR and TfR transported from TGN to CRE doubled (Figure 6A), whereas in B-KD MDCK it remained the same (Figure 6B; see values and statistical analysis in Table S3). For VSVG, the amount of protein accumulated in CRE was ~55% in WT MDCK and did not significantly increase in A-KD or B-KD MDCK cells, in agreement with the postulated obligatory *trans*-endosomal route of this protein (Ang et al., 2004; Cancino et al., 2007; Gravotta et al., 2007) (see also Figures 3E and 3F).

These results indicate that A-KD but not B-KD promote increased trafficking of LDLR and TfR from TGN to CRE, supporting a scenario in which AP-1A controls biosynthetic trafficking of PM proteins along a route independent of CRE.

Yeast Two-Hybrid Analysis of the Interactions of μ 1A and μ 1B with Basolateral Signals

As discussed in the Introduction, many basolateral proteins are sorted by signals resembling tyrosine and di-leucine endocytic motifs. One of the PM proteins characterized in this study, VSVG, displays a typical YXX Φ motif as a basolateral sorting signal (Thomas et al., 1993; Thomas and Roth, 1994). In contrast, the two other PM proteins studied here are sorted basolaterally in their biosynthetic and recycling routes by nonconventional basolateral signals distinct from endocytic motifs. For example, TfR utilizes the signal GDNS (Odorizzi and Trowbridge, 1997) whereas LDLR utilizes two basolateral signals, a “weak” proximal basolateral sorting signal (FXNPXY) and a more distal “strong” basolateral signal, GYXY (Matter et al., 1992). To date, no detailed biochemical or structural evidence is available on the interactions of these basolateral sorting signals with AP-1. Hence, we performed Y2H analysis searching for interactions with the medium subunits of this adaptor (Figure 7). Y2H analysis in plates (Figure 7A) showed interactions of both μ 1A and μ 1B with the cytoplasmic domain of TfR, but not with the cytoplasmic domains of LDLR or VSVG. Mutational analysis showed that the interaction with μ 1A was sensitive to a substitution in the YXX Φ motif-based TfR endocytic signal (Y20A) and, partially, to an *en bloc* substitution of the previously described basolateral sorting sequence of TfR (²⁹VDGDNSH) (Dargemont et al., 1993; Odorizzi and Trowbridge, 1997). In contrast, the interaction with μ 1B was impaired only by mutation of the ²⁹VDGDNSH sequence (Figure 7A). Quantitative Y2H analysis of the interaction of TfR tail constructs with μ 1A and μ 1B in liquid medium (Figure 7B) yielded

results consistent with our interpretation of the experiments carried out in plates.

These experiments demonstrate a direct interaction of the basolateral signal of TfR with the medium subunits of AP-1A and AP-1B. The inability to detect interactions of μ 1A and μ 1B with the basolateral signals of LDLR and VSVG could be due to low binding affinity, the requirement of another subunit of AP-1, or the participation of a linker protein.

DISCUSSION

We have demonstrated that the ubiquitous clathrin adaptor AP-1A plays an important role in basolateral protein trafficking. Our results are consistent with a scenario in which AP-1A operates at the TGN promoting exit of basolateral proteins along a route to the PM that avoids TfR-rich common recycling endosomes. This scenario is supported by the participation of AP-1A in the steady-state localization and biosynthetic delivery of basolateral proteins (Figures 2 and 3), the predominant localization of AP-1A to the TGN in polarized MDCK cells (Figure 4), its requirement for the exit of LDLR-GFP from TGN in live imaging experiments (Figure 5), the spillover of basolateral proteins into CRE upon AP-1A KD (Figure 6), and the ability of μ 1A to interact with the basolateral signal of TfR in yeast-two-hybrid experiments (Figure 7). The role of AP-1A in basolateral trafficking demonstrated here is complementary to that reported for AP-1B, which localizes preferentially at CRE, sorting recycling basolateral proteins and newly synthesized proteins that reach CRE after TGN exit, such as VSVG protein (Ang et al., 2004; Cancino et al., 2007; Fölsch et al., 2003; Gan et al., 2002; Gravotta et al., 2007; Mostov et al., 1999). Our data support the concept that TGN and endosomes do not operate independently in biosynthetic and recycling routes but, rather, cooperate extensively in polarized trafficking (for review, see Fölsch et al., 2009; Gonzalez and Rodriguez-Boulan, 2009; Weisz and Rodriguez-Boulan, 2009).

Our data suggest that both AP-1A and AP-1B may participate in cargo exit from the TGN as knockdown of both adaptors is required to inhibit this process (Figure 5). This is consistent with the reported ability of AP-1A to mediate Golgi exit of membrane proteins (Chi et al., 2008; Doray et al., 2002; Ma et al., 2011; Puertollano et al., 2001; Waguri et al., 2003) and with reports indicating that AP-1B can bind phosphoinositides characteristic of both CRE (i.e., PIP-3) via its μ 1B subunit (Fields et al., 2010) and TGN (i.e., PI-4P) via its γ 1 subunit (Heldwein

(D and E) Colocalization was analyzed using MCC (see Experimental Procedures). Note the high proportion (~50%) of both μ 1A-HA and μ 1B-HA that colocalized with endogenous γ -adaptin, reflecting their incorporation into the AP-1 complex. MCC 2: 0.508 ± 0.030 and 0.511 ± 0.033 , respectively ($n = 30, 33$ cells, $p > 0.95$, for μ 1A-HA and μ 1B-HA (Student's *t* test). (E) Conversely, there was also a high colocalization of γ -adaptin with μ 1A-HA or μ 1B-HA, MCC 1 0.532 ± 0.028 and 0.417 ± 0.035 , respectively ($n = 30, 33$ cells, $p > 0.013$).

(F) Values representing mean \pm SEM were derived from three independent colocalization experiments of μ 1A-HA or μ 1B-HA with TGN38- or TfR-labeled compartments. μ 1A-HA colocalized more prominently with TGN38 than μ 1B-HA (MCC 1 = 0.294 ± 0.025 and 0.094 ± 0.010 , $n = 41$ – 40 cells, respectively; $\#p < 3.5 \times 10^{-10}$, Student's *t* test). In contrast, μ 1B-HA colocalized more prominently with TfR than μ 1A-HA (MCC 1 = 0.348 ± 0.016 and 0.158 ± 0.015 , $n = 69$ and 44 cells, respectively; $[*] p < 2.8 \times 10^{-13}$, Student's *t* test).

(G) A-KD and B-KD MDCK cells, confluent for 84 hr, were fixed, immunostained for TGN38 and γ -adaptin, and analyzed by laser scanning confocal microscopy as detailed in the Supplemental Experimental Procedures. Shown in the graphs at right are the relative areas expressed as percent values, occupied by TGN38 (red line) and γ -adaptin (green line) in each confocal slice (right ordinate), numbered starting from the top of the monolayer (abscissa), along with the percent colocalization of γ -adaptin with TGN38 (brown line) in A-KD and B-KD. Note that the colocalization of γ -adaptin with TGN38, expressed as the mean \pm SD of the fraction of TGN38 area colocalized with γ -adaptin (brown line), is $34 \pm 9.8\%$ in B-KD cells and $20 \pm 3.4\%$ in A-KD cells (from $n \sim 144$ – 176 cells). The difference was statistically significant ($p < 0.0073$; Student's *t* test; bars, 15 μ m).

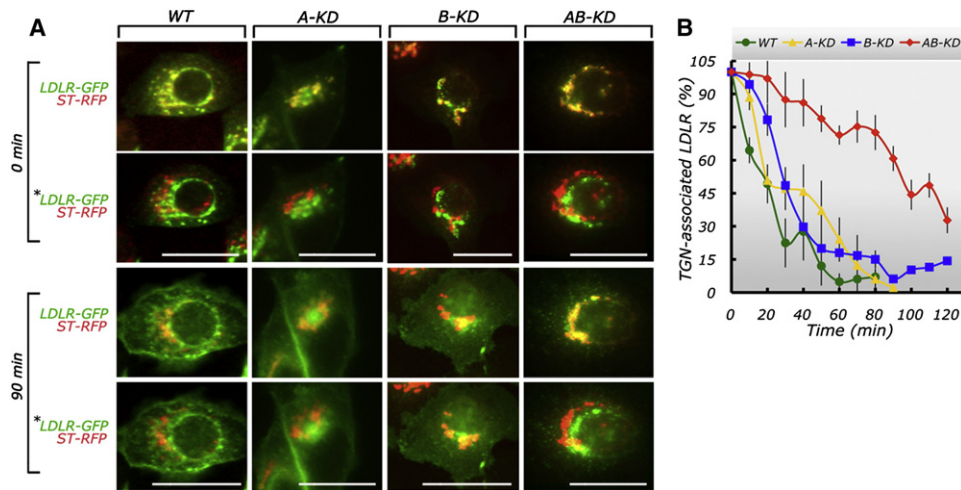


Figure 5. Double Knockdown of AP-1A and AP-1B Blocks TGN Exit of LDLR-GFP

Subconfluent control, A-KD, B-KD, or AB-KD MDCK cells, grown on glass coverslips, were microinjected with expression vectors encoding ST-RFP and LDLR-GFP, incubated at 37°C for 1 hr to allow synthesis of the protein and at 20°C for 2 hr in the presence of 100 µg/ml cycloheximide, to accumulate LDLR-GFP in the TGN. The cells were then live imaged using a 40× objective in the red and green channels (see Movie S1 and Experimental Procedures).

(A) Fluorescent imaging. Note that in control cells LDLR-GFP colocalizes with ST-RFP at chase time 0 but loses colocalization at 90 min, as LDLR-GFP exits the TGN. A similar result was observed for A-KD and B-KD MDCK cells. In AB-KD cells LDLR-GFP colocalizes to a large extent with ST-RFP at chase times 90 min, indicating that a large fraction of LDLR-GFP displayed a delayed perinuclear exit. Paired images in each panel labeled with an asterisk (*) were generated by pixel-shift of green channel, to better appreciate area of colocalization. Bar, 20 µm.

(B) Quantification of TGN exit kinetics. The figure shows the GFP/RFP fluorescence ratios at different chase times. Note that LDLR exit kinetics is not reduced in A-KD or B-KD MDCK cells but is slower in AB-KD MDCK cells. Time courses for LDLR Golgi exit were fit to a simple exponential decay model using the nonlinear least-squares function in the R software package. The time constant for AB-KD cells was determined to be 75.3 min (95% confidence interval = 64.6–87.7 min; three traces). This was significantly slower than the time constants determined for the WT cells (23.9 min, 95% confidence interval = 19.6–28.7 min; three traces), the A-KD cells (21.3 min; 95% confidence interval = 17.5–25.5 min; five traces), and the B-KD cells (29.9 min; 95% confidence interval = 27.1–32.7 min; five traces).

Data points represent mean values ± SEM computed from N > 10 obtained from two to three independent experiments.

et al., 2004). It was reported that AP-1B can compensate for lack of AP-1A in retrograde transport of man-6-P receptor (Eskelinen et al., 2002) but not furin (Fölsch et al., 2001). Our results cannot discard an apical-basolateral sorting role of AP-1A at endosomes, as there is evidence in the literature supporting a role for this adaptor in retrograde transport of mannose-6-phosphate receptors and Golgi proteins from endosomes to the TGN (Meyer et al., 2001; Robinson et al., 2010; Valdivia et al., 2002) and in anterograde transport of melanogenic enzymes from recycling endosomes to melanosomes in melanocytes (Delevoye et al., 2009; Theos et al., 2005).

We demonstrate here, using Y2H, that GDNS, the nonconventional basolateral signal of TfR interacts with both µ1A and µ1B (Figure 7). This interaction likely involves a noncanonical binding site in the µ1A and µ1B subunits, different from the hydrophobic pocket used to bind YXXΦ motifs (Owen and Evans, 1998). This is consistent with the proposal that µ1B can bind cargo through conventional and nonconventional sites (Sugimoto et al., 2002). µ1A also interacts with the endocytic signal YTRF of TfR (amino acids 20–23), fitting a YXXΦ consensus motif. The functional significance of this observation remains unclear at this time. On the other hand, we did not detect interactions of µ1A or µ1B with the well-known basolateral signals of LDLR or VSV G protein. This may reflect (1) very weak binding that cannot be detected in our Y2H analysis, (2) a piggy-back mechanism via a third protein (such a mechanism was reported for the interac-

tion of LDLR with AP-1B via its weak basolateral signal FxNPXY [Kang and Fölsch, 2011]), or (3) binding to µ1B in conjunction with other subunits of AP-1, as reported for dileucine signals and the γ-σ1 hemicomplex of AP-1 (Janvier et al., 2003). We did not observe the interaction between VSVG and µ1B reported by others (Fields et al., 2007). This may reflect a very weak interaction or, alternatively, an indirect interaction through a third protein, e.g., Eps15 (Chi et al., 2008).

The complementary roles of AP-1A and AP-1B in basolateral polarity demonstrated here highlight AP-1 as a major regulator of basolateral trafficking, a function consistent with its absolute requirement for the development of multicellular organisms (Lee et al., 1994; Zizioli et al., 1999). Future work must address the precise sorting roles of AP-1A and AP-1B and the molecular mechanisms underlying the cooperation between TGN and CRE. Understanding these mechanisms requires developing high time and space resolution live imaging assays in fully polarized epithelial cells, as well as comparative analysis of AP-1A and AP-1B interactomes, a task that has already begun (Baust et al., 2006; Fields et al., 2010).

EXPERIMENTAL PROCEDURES

Cloning and siRNA Silencing

Canine µ1A was cloned by RT-PCR with a ProStar Ultra HF RT-PCR kit (Stratagene Cedar Creek, TX), using total RNA obtained from MDCK cells

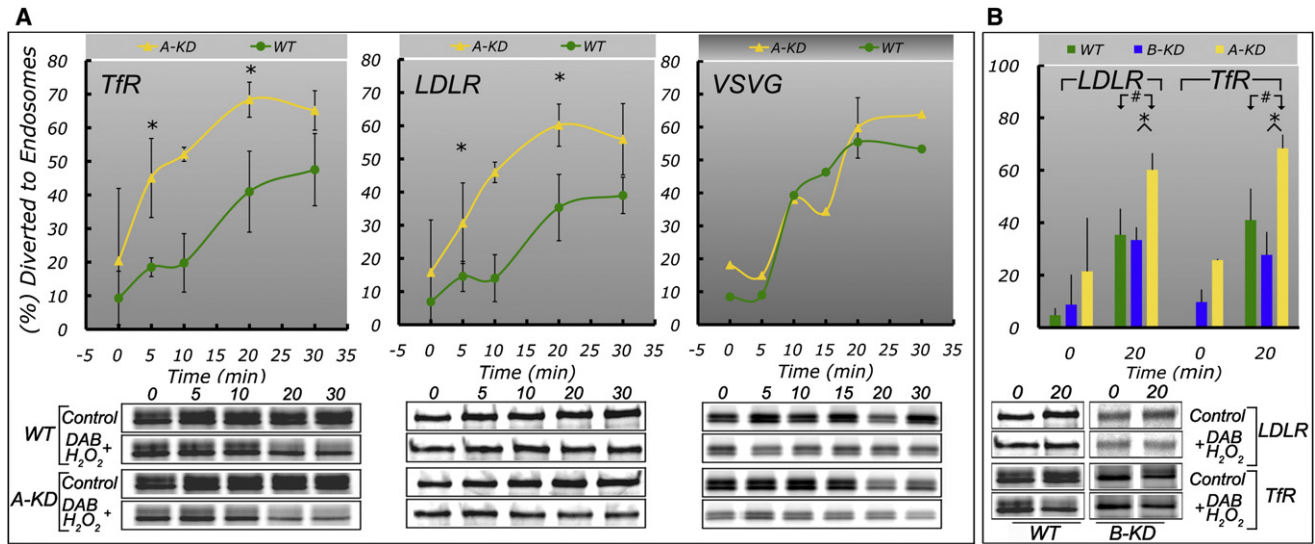


Figure 6. AP-1A Knockdown Enhances Trafficking of LDLR and TfR into CRE

Wild-type, A-KD, and B-KD MDCK cells, confluent on Transwell chambers for 54 hr were transduced either with adenoviruses encoding TfR and LDLR or with adenoviruses encoding TfR and VSVG-GFP for 26–30 hr (see *Experimental Procedures* for details). The cells were then pulsed with [³⁵S]-methionine/cysteine for 15 min, followed by a 2 hr chase at 20°C in the presence of horseradish peroxidase-conjugated transferrin (HRP-Tf) to accumulate the radioactively labeled proteins in the TGN and the HRP-Tf in recycling endosomes. Next, the cells were chased at 37°C for the indicated times, in the presence of HRP-Tf, chilled, and incubated with DAB/H₂O₂ to crosslink and trap proteins present in RE loaded with HRP-Tf. Samples were extracted, subjected to immunoprecipitation with antibodies to LDLR, TfR, or VSVG protein, and analyzed by SDS-PAGE as described in *Experimental Procedures*. The percent of the radioactively pulse-labeled proteins that became nonextractable upon HRP- and DAB/H₂O₂-induced crosslinking was calculated as the difference between control and DAB/H₂O₂-treated samples and represents the amount of cargo protein diverted into CRE.

(A) Values at each time point are average ± SEM from three independent experiments for LDLR and TfR, or from a single experiment for VSVG. Values at 0 and 20 min time points include additional experiments run in triplicates for LDLR and TfR (n = 6) and for VSVG (n = 7) in A-KD and WT MDCK cells. See *Table S3* for statistical analysis.

(B) Endosomal trafficking in A- and B-KD MDCK cells. Bars represent average ± SEM values at 0 and 20 min time points for LDLR or TfR in A- or B-KD cells from two independent experiments (n = 4). Bar values for LDLR and TfR in A-KD and WT MDCK cells are as described in (A). Note that the amounts of LDLR and TfR transported into CRE in B-KD or WT MDCK cells were not statistically different from each other. In contrast LDLR and TfR diverted into CRE in A-KD MDCK cells was significantly higher than either B-KD or WT MDCK cells. See *Table S3* for statistical analysis.

with a RNeasy mini kit (QIAGEN, Hilden, Germany) and the following set of custom synthesized primers (Sigma-Genosys The Woodlands, TX): 5'GGCC ATG TCC GCC AGC GCC GTC TAC GTG C 3' (h_μ1A-Sense) and 5'CGCGAGT GACCCAGGCTCGACATTAGAGG3' (h_μ1A-Antisense). The h_μ1A sequence obtained was used to select siRNA candidate sequences through an on line algorithm (<http://jura.wi.mit.edu/bioc/siRNAext/home.php>). Custom synthesized candidate RNAis (Dharmacon, Lafayette, CO) were tested by RT-PCR after transfection. The potent h_μ1A-targeted siRNA identified in this screening (GTGCTCATCTGCGGAATT) and a control Luciferase siRNA (GL2-siRNA) were transfected into MDCK cells by electroporation as previously described (Gravotta et al., 2007). Briefly, trypsinized cells were suspended at 4–5 × 10⁶ cells per 0.125 ml of Nucleofector Solution V (Amaxa Inc. USA), supplemented with 160 pmol of siRNA and electroporated (Program “T-23”). Cells were consecutively transfected three times at 3 day intervals. Silencing efficiency was determined by RT-PCR, with inputs of 200 ng of total RNA and by western blot analysis of total cell lysates (125 μg per track). AP-1A and AP-1B medium subunits were detected by western blot with two specific antibodies as previously described (Gravotta et al., 2007). Blots were visualized by chemiluminescence (Amersham Pharmacia Biotech, Piscataway, NJ) and quantified with ImageJ software. For experiments, the cells were seeded after the third transfection on Transwell chambers at confluency and used 3–4 days later, as indicated in the corresponding figure legends.

Domain-Selective Biotinylation and Steady-State Distribution of Membrane Proteins

The quantitative steady-state distribution of exogenous (adenovirus transduced) and endogenous membrane proteins was determined by domain-

selective surface biotinylation (Sargiacomo et al., 1989) 84 hr after seeding MDCK cells at confluency on Transwells, as previously described (Gravotta et al., 2007). Cells were rinsed twice with ice-cold Ca, Mg-HBSS and once with 25 mM triethanolamine-HCl (pH 7.8), 0.25 M sucrose, 0.5 mM Cl₂Ca, 1 mM MgCl₂ (BB) followed by two successive 20 min incubations at 4°C with 3 mg ml⁻¹ sulfo-NHS-LC-Biotin in BB, added to the apical (0.6 ml) or to the basolateral (0.3 ml) sides. Cells were rinsed twice with BB and incubated at 4°C for 20 min with 40 mM ethanolamine-HCl in BB followed by a quick rinse with Ca, Mg-free HBSS. Cells were lysed in 50 mM Tris-HCl (pH 7.4), 150 mM NaCl, 25 mM KCl, 2 mM EDTA, 1% Na-deoxycholate, 0.1% SDS, 1% Triton X-100, supplemented with 1 mM PMSF and 15 μg ml⁻¹ leupeptin/pepstatin/antipain and 37 μg ml⁻¹ benzamidin-HCl (PIC) for 30 min at 4°C. Biotinylated proteins were retrieved from lysates cleared by centrifugation (18,000 × g for 10 min) with streptavidin-Sepharose as described (Sargiacomo et al., 1989) and subjected to western blot analysis.

Quantitative Biochemical Surface Delivery Assays of PM Proteins in Their Biosynthetic and Recycling Routes

We utilized previously reported surface capture assays to assess the polarized delivery of newly synthesized transferrin receptor (Gravotta et al., 2007) and LDL receptor (Gan et al., 2002). These are surface capture assays that score the amount of cargo protein delivered to the apical or basolateral surfaces as percent of the maximum total surface (apical+basolateral) delivery (100%). For the study of VSVG protein, we introduce here a surface biotinylation-avidin-shift (SBAS) quantitative assay that scores apical and basolateral delivery of the cargo protein as a percent of total cargo protein (surface + intracellular). These assays are briefly described below.

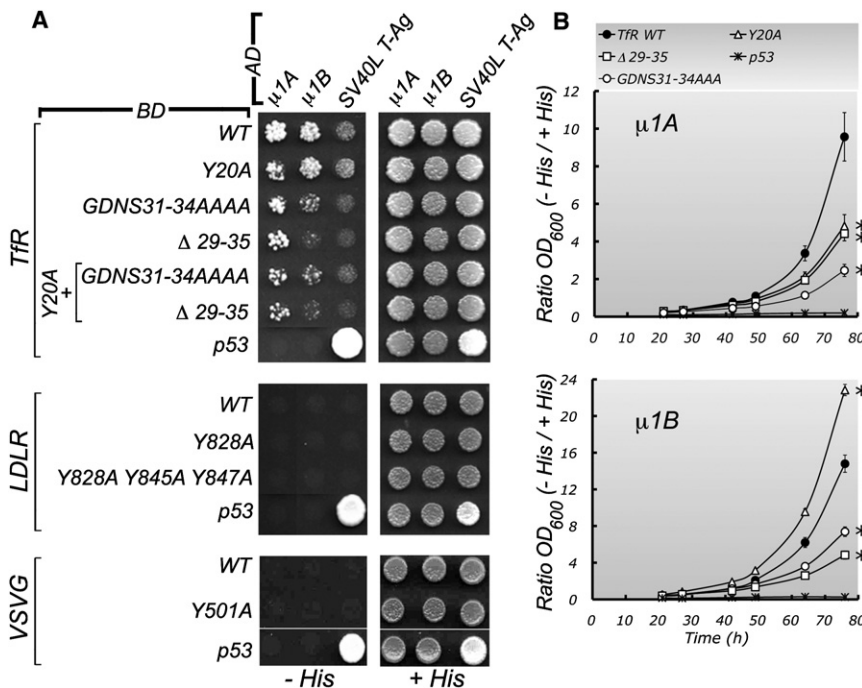


Figure 7. Yeast Two-Hybrid Analysis of Potential Interactions between μ 1A and μ 1B Subunits and the Cytoplasmic Tails of Tfr, LDLR, and VSVG

(A) Plate assays. The μ 1A/ μ 1B and the cytoplasmic tail constructs were subcloned into Y2H activation domain (AD) and binding domain (BD) vectors, respectively (see [Experimental Procedures](#) for details). Analysis of the Tfr cytoplasmic tail indicated that the interaction with μ 1A is dependent on both the YTRF sequence (amino acids 20–23; consensus motif YXX Φ) and the GDNS sequence (amino acids 31–34), while the interaction with μ 1B depends exclusively on GDNS. The lack of interaction of the human LDLR constructs with μ 1A and μ 1B subunits was also observed when the configuration of the assay was inverted by subcloning the LDLR constructs into the AD vector pGAD424 and the μ 1A and μ 1B constructs into the BD vector pGBT9 (not shown). Interaction of fusion proteins was monitored by activation of HIS3 transcription following plating of AH109 yeast strain double transformants on medium lacking His, Leu, and Trp (–His). Plating on medium lacking only Leu and Trp (+His) provided a control for growth and loading of double transformants.

(B) Liquid medium Y2H assays. Triplicate cultures in +His and –His liquid media of the different

double transformants were inoculated at high dilution (OD_{600} nm \sim 0.001) and cultured for up to 76 hr. The OD_{600} were recorded at the indicated intervals on undiluted samples or dilutions that did not exceed OD_{600} values of \sim 0.5. Results were expressed as the OD_{600} in –His medium at the indicated times divided by the OD_{600} in +His medium at 21 hr, to correct for differences in the density of the initial inocula (the OD_{600} in +His medium at 21 hr was used to avoid values exceeding the range of linearity between OD and number of cells). Growth curves of p53- μ 1A and p53- μ 1B double transformants were included as negative controls of interactions for μ 1A and μ 1B, respectively. The data shown are the means \pm SEM of triplicate growth curves for each double transformant. The data points at 64 and 76 hr were analyzed by ANOVA followed by two-tail Dunnett’s test. Asterisks at the side of the 76 hr data points indicate significant differences at $p < 0.01$ when compared to the Tfr WT tail. The same significances were obtained when analyzing the 64 hr data points with the exception of the comparison of the Tfr WT and Y20A mutant interaction with μ 1A, which was significant at $p < 0.05$ instead of $p < 0.01$ (asterisks are not shown for simplicity).

Transferrin Receptor

For Tfr, we used our recently described surface ligand capture (SLC) assay ([Gravotta et al., 2007](#)). Briefly, cells transduced with Ad-Tfr were pulse-labeled for 14 min with 0.5 mCi ml^{-1} of [^{35}S]-Protein labeling mix (EXPRE $^{35}S^{35}S$; Perkin-Elmer, Waltham, MA) followed by incubation in chase medium (serum-free DMEM supplemented with 0.75% BSA and 100 \times molar excess of methionine and cysteine) containing 50 $\mu g ml^{-1}$ biotin-Tf (B-Tf), added either to the apical or basolateral side. Excess B-Tf was washed with ice-cold Ca, Mg-HBSS 0.5% BSA (Ca, Mg-HBSS-BSA). Cells were lysed in 40 mM Na acetate (pH 5.5), 150 mM NaCl, 30 mM KCl, 2.5 mM EDTA, 1.5% Triton X-100, and 0.5% BSA (TLB [pH 5.5]) supplemented with PIC for 30 min at 4 $^{\circ}C$. The B-Tf/Tfr complex was retrieved from lysates cleared by centrifugation (18,000 $\times g$ for 10 min) after a 3 hr incubation with avidin-Sepharose followed by centrifugation (18,000 $\times g$ for 10 min). Samples were processed by SDS-PAGE and analyzed by phosphorImager. This assay was slightly modified to measure Tfr recycling, as follows: [^{35}S]-pulse-labeled cells were initially chased for 3.5 hr in chase medium to allow equilibration of newly synthesized Tfr within the endosomal compartment, prior to incubation with B-Tf, exactly as detailed above.

LDL Receptor

For LDLR, we used a surface immunocapture assay ([Gan et al., 2002](#)). Briefly, [^{35}S]-pulse-labeled cells were incubated in chase medium containing 6.5 $\mu g ml^{-1}$ rabbit anti-LDLR added either to the apical or basolateral side. Antibody excess was washed with ice-cold Ca, Mg-HBSS-BSA. Cells were lysed with 40 mM Tris-HCl (pH 7.6), 150 mM NaCl, 30 mM KCl, 2.5 mM EDTA, 1.5% Triton X-100, and 0.5% BSA supplemented with PIC (TLB [pH 7.6]) for 30 min at 4 $^{\circ}C$. The LDLR/anti-LDLR complex present in lysates, cleared by centrifugation

(18,000 $\times g$ for 10 min), was retrieved after 6 hr incubation at 4 $^{\circ}C$ with protein A-Sepharose. Samples were processed by SDS-PAGE and analyzed by phosphorImager.

VSVG

Biosynthetic delivery of this protein to apical and basolateral PM domains was measured using a SBAS assay. Cells transduced with an adenovirus encoding VSVG-GFP were pulse-labeled with [^{35}S]-methionine/cysteine, incubated in chase medium and chilled with ice-cold Ca, Mg-HBSS. Cells were subjected to domain-selective surface biotinylation as detailed above and then lysed with TLB (pH 7.6) supplemented with PIC at 4 $^{\circ}C$ for 30 min. Lysates, cleared by centrifugation (18,000 $\times g$ for 10 min), were subjected to immunoprecipitation with mouse rabbit anti-VSVG antibodies and protein G-Agarose. The immunoprecipitated protein, representing a mixture of biotinylated (surface) plus nonbiotinylated cargo protein (intracellular), was eluted by boiling samples with 40 mM Tris-HCl (pH 9.0), 1.5% SDS, and 20 mM DTT (170 μl /sample) for 10 min and divided into two identical 80 μl aliquots: (1) the first aliquot was mixed with 55 μl of avidin-shift-buffer (ASB) (500 $\mu g ml^{-1}$ avidin, 35% glycerol and 15 $\mu g ml^{-1}$ bromophenol blue); (2) the second 80 μl aliquot was mixed with 55 μl of avidin-control buffer (ACB) (1.2 mM biotin, 500 $\mu g ml^{-1}$ avidin, 35% glycerol, and 15 $\mu g ml^{-1}$ bromophenol blue). Both aliquots were incubated at 60 $^{\circ}C$ for 10 min, loaded side by side on SDS-PAGE, and quantified by phosphorImager. Under the conditions of this assay, only the biotinylated cargo protein form a tight complex with free avidin in ASB causing a shift away from its normal electrophoretic mobility into a higher molecular mass. On the other incubation with biotin-saturated avidin, ACB does not affect biotinylated and nonbiotinylated cargo protein normal electrophoretic mobility. The proportion of biotinylated protein is determined by the difference in cargo

protein determined in ACB and ASB. This assay measures independently the amount of cargo proteins delivered to the apical or basolateral cell surfaces as a percent of the total amount of cargo protein (total = surface + intracellular). Consequently, the sum of AP and BL values may be less than the total due to the intracellular fraction of the protein.

Quantitative Immunofluorescence Colocalization of μ 1A and μ 1B with TGN38 and TfR

The cellular distribution of AP-1A or AP-1B was studied by transient transfection of MDCK cells with HA-tagged μ 1A or μ 1B (μ 1A-HA, μ 1B-HA), originally provided by Heike Fölsch and Ira Mellman. MDCK cells, trypsinized from a plate seeded the day before, were suspended in 0.125 ml of Nucleofector Solution V (4×10^6 cells), added to 10 μ g of an expression vector encoding μ 1A-HA or μ 1B-HA, electroporated (Program T-23) before plating them on coverslips (2×10^4 cells/cm²). Seventy-two hours after transfection cells were fixed for 20 min with 3.5%–PFA and permeabilized with 0.075% saponin and immunolabeled with indicated antibodies as described above. Confocal images (1,040 \times 1,040) from three independent experiments were collected in a spinning-disc confocal microscope, (Zeiss Axio Observer inverted microscope equipped with a Yokogawa Confocal Scanner Unit CSU-X1 and a Photometrics Cool Snap XQ² Camera) using a Zeiss Plan APO CHROMAT 63 \times /1.46–0.60 oil-immersion objective. To quantitate the colocalization of μ 1A-HA or μ 1B-HA with TGN38, TfR or γ -adaptin-labeled compartments, we utilized the Manders' colocalization coefficient (MCC) 1 and 2 determined with Zeiss colocalization software. MCCs provide a more intuitive measure of colocalization between different cellular markers A and B, than the Pearson correlation coefficient (PCC) as they measure the fraction of A present in B (M1) and vice versa (M2), independently of signal proportionality (Dunn et al., 2011). Hence, they are ideal to measure the relative proportion of the two immunolabeled compartments of interest, such as CRE and TGN, occupied by either one of the adaptors.

Endosomal Trapping

The experimental design for endosomal trapping was adapted from earlier reports (Stoorvogel et al., 1988). A-KD, B-KD, or WT MDCK cells were cotransduced with Ad-hTfR and Ad-hLDLR or with Ad-hTfR and Ad-VSVG pairs and [³⁵S]-pulse-labeled, followed by a chase at 20°C for 2 hr in bicarbonate free medium containing 15 μ g ml⁻¹ horseradish peroxidase-conjugated transferrin (HRP-Tf). Cells were incubated at 32°C in chase medium supplemented with HRP-Tf and immediately chilled with ice-cold Ca,Mg-HBSS. Cells were incubated at 4°C with 150 μ g ml⁻¹ DAB and 0.030% H₂O₂ (v/v) in Ca,Mg-HBSS for 1 hr (crosslinked sample) or without DAB (control sample). Cells were washed with Ca,Mg-HBSS and lysed with TLB (pH 7.6) supplemented with PIC. Lysates, cleared by centrifugation (18,000 \times g for 10 min), were subjected to sequential immunoprecipitation with specific antibodies (rabbit anti-LDLR, rabbit anti-VSVG, or mouse anti-TfR) followed by SDS-PAGE and Phosphorimager analysis. The difference between control and DAB/H₂O₂-treated samples, the nonextractable protein after HRP and DAB/H₂O₂-induced crosslinking, represents the protein pool diverted into RE.

Statistical Analyses

All statistical analyses were performed in R (R: A language and environment for statistical computing, <http://www.R-project.org>). All data reported as percentages were logit transformed, and all subsequent statistics performed on the transformed values, with results reported after applying the inverse transform. Consequently, reported 95% confidence intervals are not necessarily symmetric around the mean. Single factor ANOVAs were computed with the aov function. Two-sided pairwise t tests using a pooled SD were used as posttests; reported p values were corrected for multiple hypothesis testing using either Bonferroni or Holm corrections, as indicated in the text.

SUPPLEMENTAL INFORMATION

Supplemental Information includes one figure, three tables, one movie, and Supplemental Experimental Procedures and can be found with this article online at [doi:10.1016/j.devcel.2012.02.004](https://doi.org/10.1016/j.devcel.2012.02.004).

ACKNOWLEDGMENTS

We thank Dr. Alfonso Gonzalez for reading and commenting on the manuscript. This work was supported by National Institutes of Health (NIH) grants GM34108 and EY08538 to E.R.-B., by funds from Research to Prevent Blindness Foundation, by the Dyson Foundation, and by an EMBO Postdoctoral Fellowship to J.M.C.-G. R.M. and J.S.B. were supported by the Intramural Program of the Eunice Kennedy Shriver National Institute of Child Health and Human Development, NIH. We thank B. Lelouvier (National Heart, Lung, and Blood Institute, NIH) for providing an ImageJ plugin for automated analysis of confocal images; Drs. Andres Perez-Bay, Ryan Schreiner, and Susana Salvarezza for colocalization experiments; and Luciana Gravotta, M.A., for help with statistical analyses.

Received: November 7, 2011

Revised: December 29, 2011

Accepted: February 6, 2012

Published online: May 14, 2012

REFERENCES

- Alberts, B. (2002). *Molecular Biology of the Cell*, Fourth Edition (New York: Garland Science).
- Ang, A.L., Taguchi, T., Francis, S., Fölsch, H., Murrells, L.J., Pypaert, M., Warren, G., and Mellman, I. (2004). Recycling endosomes can serve as intermediates during transport from the Golgi to the plasma membrane of MDCK cells. *J. Cell Biol.* 167, 531–543.
- Baust, T., Czupalla, C., Krause, E., Bourel-Bonnet, L., and Hoflack, B. (2006). Proteomic analysis of adaptor protein 1A coats selectively assembled on liposomes. *Proc. Natl. Acad. Sci. USA* 103, 3159–3164.
- Bonifacino, J.S., and Traub, L.M. (2003). Signals for sorting of transmembrane proteins to endosomes and lysosomes. *Annu. Rev. Biochem.* 72, 395–447.
- Bryant, D.M., and Mostov, K.E. (2008). From cells to organs: building polarized tissue. *Nat. Rev. Mol. Cell Biol.* 9, 887–901.
- Cancino, J., Torrealba, C., Soza, A., Yuseff, M.I., Gravotta, D., Henklein, P., Rodriguez-Boulan, E., and González, A. (2007). Antibody to AP1B adaptor blocks biosynthetic and recycling routes of basolateral proteins at recycling endosomes. *Mol. Biol. Cell* 18, 4872–4884.
- Chi, S., Cao, H., Chen, J., and McNiven, M.A. (2008). Eps15 mediates vesicle trafficking from the trans-Golgi network via an interaction with the clathrin adaptor AP-1. *Mol. Biol. Cell* 19, 3564–3575.
- Cresawn, K.O., Potter, B.A., Oztan, A., Guerriero, C.J., Ihrke, G., Goldenring, J.R., Apodaca, G., and Weisz, O.A. (2007). Differential involvement of endocytic compartments in the biosynthetic traffic of apical proteins. *EMBO J.* 26, 3737–3748.
- Dargemont, C., Le Bivic, A., Rothenberger, S., Iacopetta, B., and Kühn, L.C. (1993). The internalization signal and the phosphorylation site of transferrin receptor are distinct from the main basolateral sorting information. *EMBO J.* 12, 1713–1721.
- Deborde, S., Perret, E., Gravotta, D., Deora, A., Salvarezza, S., Schreiner, R., and Rodriguez-Boulan, E. (2008). Clathrin is a key regulator of basolateral polarity. *Nature* 452, 719–723.
- Delevoye, C., Hurbain, I., Tenza, D., Sibarita, J.B., Uzan-Gafso, S., Ohno, H., Geerts, W.J., Verkleij, A.J., Salameo, J., Marks, M.S., and Raposo, G. (2009). AP-1 and KIF13A coordinate endosomal sorting and positioning during melanosome biogenesis. *J. Cell Biol.* 187, 247–264.
- Diaz, F., Gravotta, D., Deora, A., Schreiner, R., Schoggins, J., Falck-Pedersen, E., and Rodriguez-Boulan, E. (2009). Clathrin adaptor AP1B controls adenovirus infectivity of epithelial cells. *Proc. Natl. Acad. Sci. USA* 106, 11143–11148.
- Doray, B., Ghosh, P., Griffith, J., Geuze, H.J., and Kornfeld, S. (2002). Cooperation of GGAs and AP-1 in packaging MPRs at the trans-Golgi network. *Science* 297, 1700–1703.

- Dunn, K.W., Kamocka, M.M., and McDonald, J.H. (2011). A practical guide to evaluating colocalization in biological microscopy. *Am. J. Physiol. Cell Physiol.* **300**, C723–C742.
- Dwyer, N.D., Adler, C.E., Crump, J.G., L'Etoile, N.D., and Bargmann, C.I. (2001). Polarized dendritic transport and the AP-1 mu1 clathrin adaptor UNC-101 localize odorant receptors to olfactory cilia. *Neuron* **31**, 277–287.
- Eskelinen, E.L., Meyer, C., Ohno, H., von Figura, K., and Schu, P. (2002). The polarized epithelia-specific mu 1B-adaptin complements mu 1A-deficiency in fibroblasts. *EMBO Rep.* **3**, 471–477.
- Fields, I.C., Shteyn, E., Pypaert, M., Proux-Gillardeaux, V., Kang, R.S., Galli, T., and Fölsch, H. (2007). v-SNARE cellubrevin is required for basolateral sorting of AP-1B-dependent cargo in polarized epithelial cells. *J. Cell Biol.* **177**, 477–488.
- Fields, I.C., King, S.M., Shteyn, E., Kang, R.S., and Fölsch, H. (2010). Phosphatidylinositol 3,4,5-trisphosphate localization in recycling endosomes is necessary for AP-1B-dependent sorting in polarized epithelial cells. *Mol. Biol. Cell* **21**, 95–105.
- Fölsch, H., Ohno, H., Bonifacino, J.S., and Mellman, I. (1999). A novel clathrin adaptor complex mediates basolateral targeting in polarized epithelial cells. *Cell* **99**, 189–198.
- Fölsch, H., Pypaert, M., Schu, P., and Mellman, I. (2001). Distribution and function of AP-1 clathrin adaptor complexes in polarized epithelial cells. *J. Cell Biol.* **152**, 595–606.
- Fölsch, H., Pypaert, M., Maday, S., Pelletier, L., and Mellman, I. (2003). The AP-1A and AP-1B clathrin adaptor complexes define biochemically and functionally distinct membrane domains. *J. Cell Biol.* **163**, 351–362.
- Fölsch, H., Mattila, P.E., and Weisz, O.A. (2009). Taking the scenic route: biosynthetic traffic to the plasma membrane in polarized epithelial cells. *Traffic* **10**, 972–981.
- Gan, Y., McGraw, T.E., and Rodriguez-Boulant, E. (2002). The epithelial-specific adaptor AP1B mediates post-endocytic recycling to the basolateral membrane. *Nat. Cell Biol.* **4**, 605–609.
- Gonzalez, A., and Rodriguez-Boulant, E. (2009). Clathrin and AP1B: key roles in basolateral trafficking through trans-endosomal routes. *FEBS Lett.* **583**, 3784–3795.
- Gravotta, D., Deora, A., Perret, E., Oyanadel, C., Soza, A., Schreiner, R., Gonzalez, A., and Rodriguez-Boulant, E. (2007). AP1B sorts basolateral proteins in recycling and biosynthetic routes of MDCK cells. *Proc. Natl. Acad. Sci. USA* **104**, 1564–1569.
- Heldwein, E.E., Macia, E., Wang, J., Yin, H.L., Kirchhausen, T., and Harrison, S.C. (2004). Crystal structure of the clathrin adaptor protein 1 core. *Proc. Natl. Acad. Sci. USA* **101**, 14108–14113.
- Henry, L., and Sheff, D.R. (2008). Rab8 regulates basolateral secretory, but not recycling, traffic at the recycling endosome. *Mol. Biol. Cell* **19**, 2059–2068.
- Janvier, K., Kato, Y., Boehm, M., Rose, J.R., Martina, J.A., Kim, B.Y., Venkatesan, S., and Bonifacino, J.S. (2003). Recognition of dileucine-based sorting signals from HIV-1 Nef and LIMP-II by the AP-1 gamma-sigma1 and AP-3 delta-sigma3 hemicomplexes. *J. Cell Biol.* **163**, 1281–1290.
- Kang, R.S., and Fölsch, H. (2011). ARH cooperates with AP-1B in the exocytosis of LDLR in polarized epithelial cells. *J. Cell Biol.* **193**, 51–60.
- Kelly, B.T., McCoy, A.J., Späte, K., Miller, S.E., Evans, P.R., Höning, S., and Owen, D.J. (2008). A structural explanation for the binding of endocytic dileucine motifs by the AP2 complex. *Nature* **456**, 976–979.
- Lee, J., Jongeward, G.D., and Sternberg, P.W. (1994). unc-101, a gene required for many aspects of *Caenorhabditis elegans* development and behavior, encodes a clathrin-associated protein. *Genes Dev.* **8**, 60–73.
- Ma, D., Taneja, T.K., Hagen, B.M., Kim, B.Y., Ortega, B., Lederer, W.J., and Welling, P.A. (2011). Golgi export of the Kir2.1 channel is driven by a trafficking signal located within its tertiary structure. *Cell* **145**, 1102–1115.
- Matter, K., Hunziker, W., and Mellman, I. (1992). Basolateral sorting of LDL receptor in MDCK cells: the cytoplasmic domain contains two tyrosine-dependent targeting determinants. *Cell* **71**, 741–753.
- Mellman, I., and Nelson, W.J. (2008). Coordinated protein sorting, targeting and distribution in polarized cells. *Nat. Rev. Mol. Cell Biol.* **9**, 833–845.
- Meyer, C., Zizioli, D., Lausmann, S., Eskelinen, E.L., Hamann, J., Saftig, P., von Figura, K., and Schu, P. (2000). mu1A-adaptin-deficient mice: lethality, loss of AP-1 binding and rerouting of mannose 6-phosphate receptors. *EMBO J.* **19**, 2193–2203.
- Meyer, C., Eskelinen, E.L., Guruprasad, M.R., von Figura, K., and Schu, P. (2001). Mu 1A deficiency induces a profound increase in MPR300/IGF-II receptor internalization rate. *J. Cell Sci.* **114**, 4469–4476.
- Moreno, J.H., and Diamond, J.M. (1974). Discrimination of monovalent inorganic cations by “tight” junctions of gallbladder epithelium. *J. Membr. Biol.* **15**, 277–318.
- Mostov, K., ter Beest, M.B., and Chapin, S.J. (1999). Catch the mu1B train to the basolateral surface. *Cell* **99**, 121–122.
- Odorizzi, G., and Trowbridge, I.S. (1997). Structural requirements for basolateral sorting of the human transferrin receptor in the biosynthetic and endocytic pathways of Madin-Darby canine kidney cells. *J. Cell Biol.* **137**, 1255–1264.
- Ohno, H., Tomemori, T., Nakatsu, F., Okazaki, Y., Aguilar, R.C., Foelsch, H., Mellman, I., Saito, T., Shirasawa, T., and Bonifacino, J.S. (1999). Mu1B, a novel adaptor medium chain expressed in polarized epithelial cells. *FEBS Lett.* **449**, 215–220.
- Owen, D.J., and Evans, P.R. (1998). A structural explanation for the recognition of tyrosine-based endocytotic signals. *Science* **282**, 1327–1332.
- Philp, N., Shoshani, L., Cerejido, M., and Rodriguez-Boulant, E. (2011). Epithelial domains. In *Membrane domains*, R. Nabi, ed. (Hoboken, NJ: Wiley).
- Puertollano, R., Aguilar, R.C., Gorshkova, I., Crouch, R.J., and Bonifacino, J.S. (2001). Sorting of mannose 6-phosphate receptors mediated by the GGAs. *Science* **292**, 1712–1716.
- Robinson, M.S., Sahlender, D.A., and Foster, S.D. (2010). Rapid inactivation of proteins by rapamycin-induced rerouting to mitochondria. *Dev. Cell* **18**, 324–331.
- Rodriguez-Boulant, E., Kreitzer, G., and Müsch, A. (2005). Organization of vesicular trafficking in epithelia. *Nat. Rev. Mol. Cell Biol.* **6**, 233–247.
- Sargiacomo, M., Lisanti, M., Graeve, L., Le Bivic, A., and Rodriguez-Boulant, E. (1989). Integral and peripheral protein composition of the apical and basolateral membrane domains in MDCK cells. *J. Membr. Biol.* **107**, 277–286.
- Schreiner, R., Frindt, G., Diaz, F., Carvajal-Gonzalez, J.M., Perez Bay, A.E., Palmer, L.G., Marshansky, V., Brown, D., Philp, N.J., and Rodriguez-Boulant, E. (2010). The absence of a clathrin adapter confers unique polarity essential to proximal tubule function. *Kidney Int.* **78**, 382–388.
- Simmen, T., Höning, S., Icking, A., Tikkanen, R., and Hunziker, W. (2002). AP-4 binds basolateral signals and participates in basolateral sorting in epithelial MDCK cells. *Nat. Cell Biol.* **4**, 154–159.
- Stoorvogel, W., Geuze, H.J., Griffith, J.M., and Strous, G.J. (1988). The pathways of endocytosed transferrin and secretory protein are connected in the trans-Golgi reticulum. *J. Cell Biol.* **106**, 1821–1829.
- Sugimoto, H., Sugahara, M., Fölsch, H., Koide, Y., Nakatsu, F., Tanaka, N., Nishimura, T., Furukawa, M., Mullins, C., Nakamura, N., et al. (2002). Differential recognition of tyrosine-based basolateral signals by AP-1B subunit mu1B in polarized epithelial cells. *Mol. Biol. Cell* **13**, 2374–2382.
- Takahashi, D., Hase, K., Kimura, S., Nakatsu, F., Ohmae, M., Mandai, Y., Sato, T., Date, Y., Ebisawa, M., Kato, T., et al. (2011). The epithelia-specific membrane trafficking factor AP-1B controls gut immune homeostasis in mice. *Gastroenterology* **141**, 621–632.
- Theos, A.C., Tenza, D., Martina, J.A., Hurbain, I., Peden, A.A., Sviderskaya, E.V., Stewart, A., Robinson, M.S., Bennett, D.C., Cutler, D.F., et al. (2005). Functions of adaptor protein (AP)-3 and AP-1 in tyrosinase sorting from endosomes to melanosomes. *Mol. Biol. Cell* **16**, 5356–5372.
- Thomas, D.C., and Roth, M.G. (1994). The basolateral targeting signal in the cytoplasmic domain of glycoprotein G from vesicular stomatitis virus resembles a variety of intracellular targeting motifs related by primary sequence but having diverse targeting activities. *J. Biol. Chem.* **269**, 15732–15739.
- Thomas, D.C., Brewer, C.B., and Roth, M.G. (1993). Vesicular stomatitis virus glycoprotein contains a dominant cytoplasmic basolateral sorting signal critically dependent upon a tyrosine. *J. Biol. Chem.* **268**, 3313–3320.

Traub, L.M. (2009). Tickets to ride: selecting cargo for clathrin-regulated internalization. *Nat. Rev. Mol. Cell Biol.* 10, 583–596.

Valdivia, R.H., Baggott, D., Chuang, J.S., and Schekman, R.W. (2002). The yeast clathrin adaptor protein complex 1 is required for the efficient retention of a subset of late Golgi membrane proteins. *Dev. Cell* 2, 283–294.

Waguri, S., Dewitte, F., Le Borgne, R., Rouillé, Y., Uchiyama, Y., Dubremetz, J.F., and Hoflack, B. (2003). Visualization of TGN to endosome trafficking

through fluorescently labeled MPR and AP-1 in living cells. *Mol. Biol. Cell* 14, 142–155.

Weisz, O.A., and Rodriguez-Boulan, E. (2009). Apical trafficking in epithelial cells: signals, clusters and motors. *J. Cell Sci.* 122, 4253–4266.

Zizioli, D., Meyer, C., Guhde, G., Saftig, P., von Figura, K., and Schu, P. (1999). Early embryonic death of mice deficient in gamma-adaptin. *J. Biol. Chem.* 274, 5385–5390.